

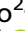





RESEARCH ARTICLE

Microdeletion in distal *PLP1* enhancers causes hereditary spastic paraplegia 2

Xun Zhou¹ , Yige Wang² , Runcheng He², Zhenhua Liu^{2,3,4}, Qian Xu^{2,3,4}, Jifeng Guo^{2,3,4} , Xinxiang Yan^{2,3}, Jinchen Li^{1,2,3,5} , Beisha Tang^{1,2,3,4} , Sheng Zeng⁶ & Qiying Sun^{1,3,4} 

¹Department of Geriatric Neurology, Xiangya Hospital, Central South University, Changsha, China

²Department of Neurology, Xiangya Hospital, Central South University, Changsha, China

³National Clinical Research Center for Geriatric Disorders, Xiangya Hospital, Central South University, Changsha, China

⁴Key Laboratory of Hunan Province in Neurodegenerative Disorders, Central South University, Changsha, China

⁵Center for Medical Genetics, School of Life Sciences, Central South University, Changsha, China

⁶Department of Geriatrics, The Second Xiangya Hospital, Central South University, Changsha, China

Correspondence

Qiying Sun, Department of Geriatric Neurology, Xiangya Hospital, Central South University, Changsha, Hunan 410008, China.
Tel: 0731-89753752; Fax: 0731-4327332;
E-mail: sunqiying2015@163.com

Sheng Zeng, Department of Geriatrics, The Second Xiangya Hospital, Central South University, Changsha, Hunan 410011, China.
Tel: 0731-85294321; Fax: 0731-85294321;
E-mail: zengsheng51314@163.com

Received: 29 January 2023; Revised: 26 June 2023; Accepted: 27 June 2023

Annals of Clinical and Translational Neurology 2023; 10(9): 1590–1602

doi: 10.1002/acn3.51848

Abstract

Objectives: Hereditary spastic paraplegia (HSP) is a genetically heterogeneous disease caused by over 70 genes, with a significant number of patients still genetically unsolved. In this study, we recruited a suspected HSP family characterized by spasticity, developmental delay, ataxia and hypomyelination, and intended to reveal its molecular etiology by whole exome sequencing (WES) and long-read sequencing (LRS) analyses. **Methods:** WES was performed on 13 individuals of the family to identify the causative mutations, including analyses of SNVs (single-nucleotide variants) and CNVs (copy number variants). Accurate circular consensus (CCS) long-read sequencing (LRS) was used to verify the findings of CNV analysis from WES. **Results:** SNVs analysis identified a missense variant c.195G>T (p.E65D) of *MORF4L2* at Xq22.2 co-segregating in this family from WES data. Further CNVs analysis revealed a microdeletion, which was adjacent to the *MORF4L2* gene, also co-segregating in this family. LRS verified this microdeletion and confirmed the deletion range (chrX: 103,690,507–103,715,018, hg38) with high resolution at nucleotide level accuracy. **Interpretations:** In this study, we identified an Xq22.2 microdeletion (about 24.5 kb), which contains distal enhancers of the *PLP1* gene, as a likely cause of SPG2 in this family. The lack of distal enhancers may result in transcriptional repression of *PLP1* in oligodendrocytes, potentially affecting its role in the maintenance of myelin, and causing SPG2 phenotype. This study has highlighted the importance of noncoding genomic alterations in the genetic etiology of SPG2.

Introduction

Hereditary spastic paraplegia (HSP) is a genetically and clinically heterogeneous group of inherited neurodevelopmental or neurodegenerative diseases, with a prevalence of one to ten per 100,000 individuals worldwide.¹ The core clinical manifestations include spasticity of lower extremities, hyperreflexia, and extensor plantar reflexes.² HSPs are clinically categorized as pure and complicated forms. The pure form is generally limited to lower extremities spasticity, with or without urinary symptoms or sensory dysfunction. The complicated form of HSP is

associated with additional manifestations such as intellectual disability, peripheral neuropathy, seizures, visual abnormality, ataxia, etc.^{3,4} To date, there are more than 70 genes that have been described to be associated with HSP. All inheritance patterns were involved in HSP, including Mendelian (autosomal dominant, autosomal recessive, and X-linked) and non-Mendelian (mitochondrial transmission). However, there are still a considerable number of genetically unsolved patients.

The *PLP1* gene is located at Xq22.2 and is responsible for encoding proteolipid protein 1, an abundant membrane protein found in the myelin of the central neural

system (CNS).⁵ Notably, *PLP1* exhibits dosage sensitivity, resulting in disease traits by copy number gains and losses. Compared to duplications or point mutations, *PLP1* null mutations are known to manifest with milder neurological symptoms. These mutations are often accompanied by peripheral neuropathy and are most commonly associated with hereditary spastic paraplegia 2 (SPG2).⁶

Recent advances in novel sequencing technology allow entire DNA sequences to be queried for disease-causing genetic variants, including noncoding regions. Noncoding sequences are segments of the genome that do not encode proteins, but they play crucial roles in gene regulation. Because Pelizaeus–Merzbacher disease (PMD)/SPG2 can result from overexpression or under-expression, proper regulation of *PLP1* expressions is physiologically significant. Enhancers are regulatory elements that can activate the expression of nearby genes, and several enhancer mutations have been linked to congenital disorders.⁷ A recent study identified two distal *PLP1* enhancers, EC1 and EC2, located between *MORF4L2* and *GLRA4*, and experimentally validated them as oligodendrocyte-specific transcription of *PLP1* gene.⁸

Herein, we reported the clinical manifestations of a family affected by hereditary SPG2, and identified the deletion of distal enhancers of *PLP1* as a likely genetic cause of SPG2 in this family. We also provided a summary and comparison of the genotype–phenotype correlations between our patients and other individuals with null *PLP1* mutations.

Methods

Participants

Two affected individuals and 11 healthy unaffected members from a Chinese family were included in this study (Fig. 1A). All individuals were subjected to thorough neurological examinations by at least two experienced neurologists. Brain and spinal MRIs were performed in all 13 family members, and the brainstem auditory evoked potentials (BAEP) and nerve conduction study (NCS) were performed in the two affected individuals. The severity of spastic paraplegia was evaluated by the Spastic Paraplegia Rating Scale (SPRS). The cognition was assessed by Mini-Mental State Examination (MMSE), Clinical Dementia Rating (CDR), and Neuropsychiatric Inventory (NPI). Genomic DNA was extracted from peripheral blood leucocytes using QIAamp DNA Mini Kit/DNeasy Plant Mini Kit[®] (QIAGEN). The project was approved by Xiangya Hospital, Central South University. Informed consents were obtained from the proband and other family members involved in this study.

Whole exome sequencing and multiplex ligation-dependent probe amplification

Whole exome sequencing (WES) was performed to detect potential causal single-nucleotide variants (SNVs) in all 13 individuals (I-1, I-2, I-3, I-4, II-1, II-2, II-3, II-4, II-5, II-6, II-7, III-1, and III-2). The exome sequences were efficiently enriched from 0.4 µg genomic DNA using Agilent liquid capture system (Agilent SureSelect Human All Exon V6) according to the manufacturer's protocol, with 2 × 150 bp sequencing mode. The sequencing data used the BWA-GATK-ANNOVAR analysis pipeline. Burrows–Wheeler Aligner (BWA) was performed to align the reads to human reference genome (GCRH37/hg19). Genome Analysis Toolkit (GATK) was used for variant calling and filtering, and the variants were annotated using ANNOVAR. The classification of variants was according to the guidelines of the American College of Medical Genetics and Genomics (ACMG).

The multiplex ligation-dependent probe amplification (MLPA) kit (SALSA MLPA probemix P165 and P213, MRC-Holland) was used to detect the extent of large deletions or duplications of several spastic paraplegia associated genes, including *SPAST*, *ATL1*, *REEP1*, and *SPG7*. MLPA results were analyzed by Coffalyer.net software.

Long-read whole genome sequencing

LRS was performed to further detect the potential structural variants in III-1. The integrity of the DNA was determined with the Agilent 4200 Bioanalyzer (Agilent Technologies, Palo Alto, California). Fifteen micrograms of genomic DNA were sheared using g-Tubes (Covaris), and concentrated using AMPure PB magnetic beads. Each SMRT bell library was constructed by SMRTbell express template prep kit 2.0 (Pacific Biosciences). The libraries were size-selected on a BluePippin[™] system for molecules ≥11 kb, followed by primer annealing and SMRT bell templates binding to polymerases using the DNA/polymerase binding kit. Sequencing was carried out on the Pacific Bioscience Sequel II platform for 30 h. Long reads were aligned to the reference genome (GRCh38/hg38) using NGMLR. Structural variations (SVs) were detected by sniffles and annotation by ANNOVAR.

Polymerase chain reaction

PCR was used to verify the breakpoint from long-read sequencing. Forward primer (5'-ACCTGGATAATTCCTGG-CATA-3') and reverse primer were designed (5'-GGACT-GAGGGATGGTGAATG-3') to span the deletion. Intronic primers were designed for the PCR amplification to cover

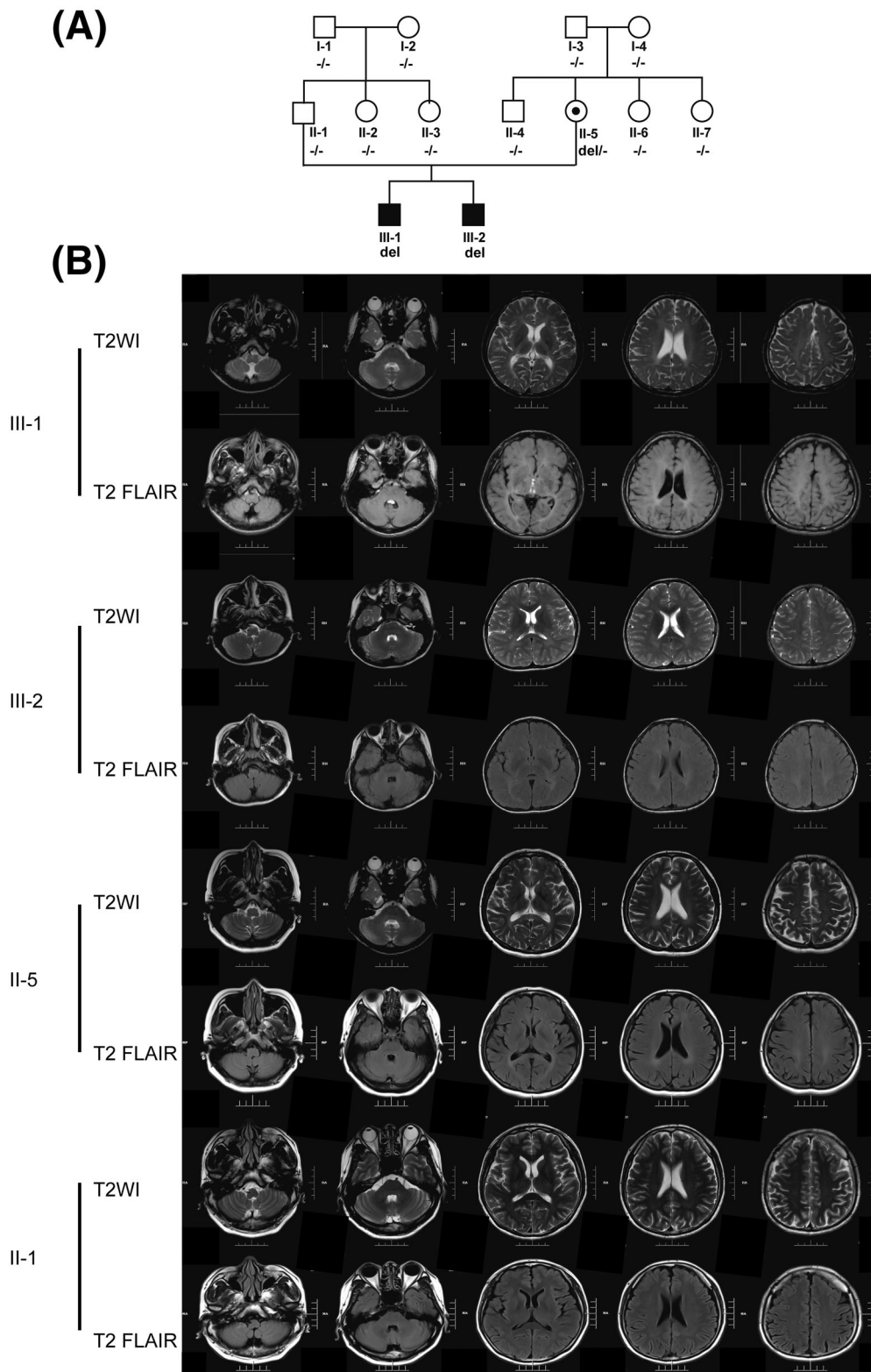


Figure 1. (A) Family tree. (B) T2-weighted image (T2WI) and fluid-attenuated inversion recovery (FLAIR) revealed symmetric, diffuse hyperintensity in the periventricular white matter and the posterior limbs of the internal capsule in III-1, III-2, and II-5. Brain atrophy is shown in III-1, and II-5 presented normal brain MRI.

the whole intron 3 of *PLP1* gene to exclude the hypomyelination of early myelinating structures (HEMS) causing alteration (Intron3-A, 5'-CTCATTCTTTGGAGCGGGTG-3' and 5'-ATTGCTGGAACCCACACATG-3', Intron3-B, 5'-CCATGCTTTGAGTGAGGTGC-3' and 5'-AAGCACCCGTACCCTAACTC-3'). The following thermal conditions were used: initial denaturation at 94°C for 1 min, followed by 30 cycles for 94°C for 30 s, 62°C for 30 s, and 72°C for 2 min. The PCR products were analyzed by electrophoresis on a 1.2% agarose gel and Sanger sequencing.

Results

Clinical findings in the investigated family

The clinical features of individuals affected by microdeletion were summarized in Table 1. The proband (III-1) is an 18-year-old man who was born after normal pregnancy and delivery. While his infantile development was normal, his parents observed delays in his motor development, including poor jumping and running ability at the age of 2 years. At the age of 6 years, he demonstrated poor learning and athletic ability compared to his peers. Furthermore, at 8 years old, he developed a spastic gait, poor coordination, and dysarthria, which progressively worsened. He did not show any signs of epilepsy or extrapyramidal signs. He has reported poor eyesight since childhood, and his ophthalmoscope revealed optic atrophy. At 18 years old, he was admitted to our hospital. His eye movements were not restricted, and nystagmus was detected. Neurologic examinations of his lower extremities showed hyperactive reflexes and extensor plantar reflexes. Motor-evoked potential (MEP) tests were abnormal in the upper and lower extremities. The brain magnetic resonance image (MRI) showed atrophy and hyperintensity in the cerebral white matter (Fig. 1B). His 8-year-old younger brother (III-2) had similar phenotypes and MRI also revealed hyperintensity (Fig. 1B). Although their parents did not report any abnormal clinical phenotypes, the neurological examination of the proband's mother (II-5) revealed hyperactive reflexes in both lower extremities and induced extensor plantar reflexes. Additionally, the brain MRI of the proband's mother (II-5) also showed abnormal hyperintensity in the white matter (Fig. 1B). Both her parents (I-3 and I-4), and other family members (I-1, I-2, II-1, II-2, II-3, II-4, II-6, and II-7) showed normal brain MRI.

Whole exome sequencing

WES and MLPA did not reveal any known causative genes for HSP. WES revealed a missense variant c.195G>T (p.E65D) in *MORF4L2* (GCRh37/hg19), which

co-segregated in three affected individuals but not in 10 unaffected members, with MAF <0.001 in East Asian (EAS) populations of the ExAC, GnomAD genome, GnomAD exome, and our in-house database. In silico damage prediction was conducted using multiple metrics evaluation, including the ReVe score (score 0.136),⁹ CADD PHRED score (score 9.099), REVEL rank score (score 0.014), and SIFT score (score 0.319). *MORF4L2* is located on Xq22.2 and encodes mortality factor 4-like protein 2, a component of the NuA4 histone acetyltransferase complex that is involved in transcriptional activation. *MORF4L2* is expressed in over 200 tissues, including brain tissue. As Xq22 is known for its genomic instability, we performed CNV (copy number variation) analysis in this region. The brothers (III-1 and III-2) and their mother (II-5) shared a single CNV, which was a deletion of the *GLRA4* and *TMEM31* gene, just located adjacent to *MORF4L2*. The variant c.195G>T (p.E65D) in *MORF4L2* gene is possibly linked to this CNV. Evaluation of the BAM file showed hemizygous deletion of the siblings, and possibly heterozygous deletion of their mother (II-5) (Supporting Information Figure S1). However, the deletion range and breakpoint were not available from the WES data.

Long-read whole genome sequencing successfully detected the mutation

As the deletion range and breakpoint could not be accurately identified by WES, we performed long-read whole genome sequencing on the PacBio Sequel platform to investigate potential complex SVs. Within the suspected region, we did observe a microdeletion of 24,512 bp at Xq22.2 (chrX: 103,690,507–103,715,018, GCRh38/hg38) in patient III-1 (Fig. 2B–D), supported by all reads with a high-resolution deletion breakpoint. This microdeletion partially involved one antisense RNA (asRNA) and two genes: *MORF4L2-AS1* (exon 1 deletion), *GLRA4* (exon1 and exon 2 deletions), and *TMEM31* (exon 8 and exon9 deletions) (Fig. 2A). By aligning the sequences to the reference genome, we obtained complete information on the breakpoint junctions and the flanking regions. Moreover, we identified a 5 bp (AGACA) microhomology region at the breakpoint (Figs. 2D and E, 3B and C). Then we analyzed the sequence flanking of each breakpoint, but we did not observe any inversion or duplication at the breakpoint or flanking sequence.

Variant verification

We conducted PCR and Sanger sequencing to validate the breakpoint of the deletion and confirm the results of long-read sequencing. The electrophoresis on a 1.2%

Table 1. The clinical characteristics of a family affected by hereditary SPG2.

Clinical features	III-1	III-2	II-5
Gender	Male	Male	Female
Age at onset, yrs	2	2	–
Current age, yrs	18	8	–
UL/LL spasticity	–/+	–/+	–/–
UL/LL weakness	–/–	–/–	–/–
Visual system	Refractive anomaly	Refractive anomaly	–
Cognitive function	MCI	MCI	Normal
Developmental delay	+	+	–
Gastrointestinal	–	–	–
Urinary/fecal urgency or incontinence	–	–	–
Extensor plantar reflex	+	+	+
Hyperactive reflexes	+	+	+
Sensory deficits	–	–	–
Dysarthria	+	+	–
Ataxia	+	+	–
Muscle atrophy	–	–	–
Seizure	–	–	–
Retinopathy	–	–	–
Deafness	–	–	–
Optic atrophy	+	+	–
Nystagmus	+	+	–
Extrapyramidal involvement	–	–	–
Pain	–	–	–
Behavior abnormal	–	–	–
Facial dysmorphism	–	–	–
SPRS	16	8	NA
Brain MRI	Symmetric and diffuse hyperintensity in the periventricular white matter and the posterior limbs of the internal capsule	Symmetric and diffuse hyperintensity in the periventricular white matter and the posterior limbs of the internal capsule	Mild hyperintensity in the periventricular white matter and the posterior limbs of the internal capsule
Spinal cord MRI	–	–	–
Peripheral neuropathy	Normal	Normal	NA
MEP	+	+	NA
SEP	–	–	NA
VEP	+	+	NA
MMSE	23	NA	27
CDR	0.5	NA	0
NPI	0	NA	0

Abbreviations: CDR, Clinical Dementia Rating; LL, lower limb; MCI, mild cognitive impairment; MEP, motor-evoked potentials; MMSE, Mini-Mental State Examination; NA, not available; NCS, nerve conduction studies; NPI, Neuropsychiatric Inventory; SEP, sensory-evoked potentials; UL, upper limb; VEP, visual evoked potentials.

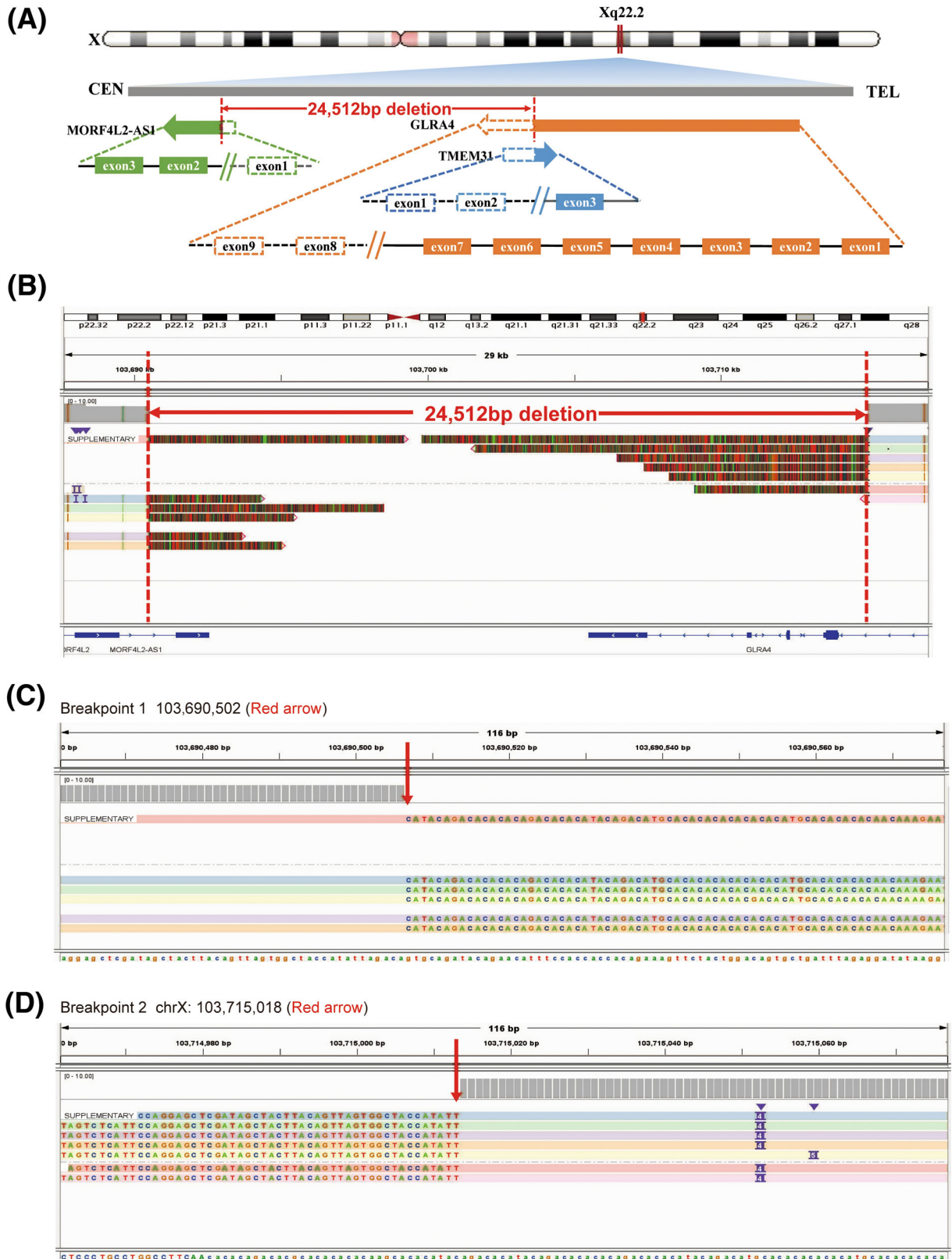


Figure 2. (A) Diagrammatic sketch of the deletion. (B) The deletion shown in Integrative Genomics Viewer (IGV) from the original BAM file of the proband. (C, D) The breakpoint (red arrow) of deletion.

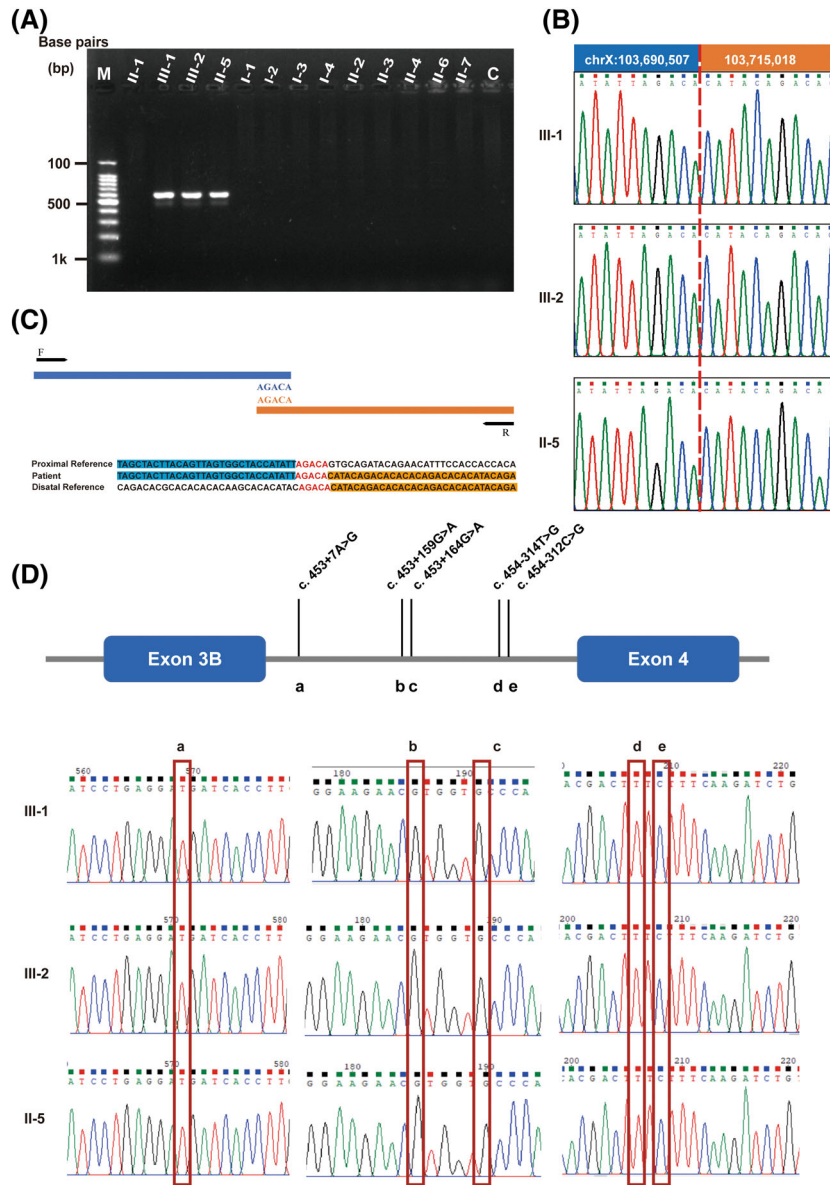


Figure 3. (A) Confirmation of the deletion of the genes by agarose gel electrophoresis of PCR products. Chromosomal DNA of the mutant strains served as the template for PCR (III-1, III-2, and II-5). Fragments of the wild type strain were too long to obtain PCR products. (B) Validation of the breakpoints by Sanger sequencing. (C) Sequence data for the breakpoint junction and microhomologies are marked in red letter. Proximal reference is marked in blue, and distal reference is marked in orange. (D) There were no alterations in regions wherein previously reported as HEMS-causing mutations.

agarose gel of PCR products showed lanes of approximately 560 bp in II-5, III-1, and III-2, while no fragments were detected in other unaffected family members due to the long fragment sizes from the wild type. (Fig. 3A). This deletion was inherited from the asymptomatic mother (II-5) and was a de novo origin in II-5. Results from Sanger sequencing were consistent with those of LRS (Fig. 3B). No variants were detected in intron 3 of the *PLP1* gene by Sanger sequencing (Fig. 3D).

Discussion

In the present study, we reported a family with hereditary SPG2 and identified a novel microdeletion of 24.5 kb at Xq22.2 co-segregated in this family. This microdeletion is located between *MORF4L2* and *GLRA4* and contains two distal enhancers of the *PLP1* gene reported previously.⁸ Although there was a missense variant (*MORF4L2* c.195G>T) revealed by SNV analysis in this family, it was considered uncertain significance according to ACMG.

Table 2. The clinical features of patients with *PLP1* null mutations.

Clinical features	Patient A					Patient 1	Patient 2	Patient 3	Patient 3		
	III-1	III-2	BAB1379	BAB1684	Patient A	(II-1)	(II-2)	(I-1)	Patient 1	Patient 2	Patient 3
Classified type	SPG2	SPG2	SPG2	SPG2	SPG2	SPG2	SPG2	SPG2	EONDT	EONDT	EONDT
Gender	Male	Male	Male	Male	Male	Male	Female	Female	Female	Female	Female
Current age, yrs	18	8	10	10	2	29	31	59	3	7	19
Spasticity	+	+	+	+	+	+	+	+	–	–	–
Intellectual development/ cognitive function	MCI	MCI	NA	Severe delay	NA	NA	–	Dementia	Severe delay	Severe delay	Severe delay
Motor development	Moderate delay	Moderate delay	Severe delay	Severe delay	Moderate delay	Moderate delay	Moderate delay	Almost normal	Severe delay	Severe delay	Severe delay
Eyes	Refractive anomaly, nystagmus, optic atrophy	Refractive anomaly, nystagmus, optic atrophy	NA	–	–	–	Nystagmus	Nystagmus	Strabismus	Divergent strabismus	–
Gastrointestinal	–	–	NA	NA	NA	NA	NA	NA	Gastroesophageal reflux	–	Constipation
Dysarthria	–	–	NA	+	+	+	–	–	+	+	+
Dysphagia	+	+	NA	–	NA	+	+	–	+	–	–
Ataxia	+	+	NA	NA	+	+	–	–	NA	NA	NA
Abnormal behaviors	–	–	NA	NA	NA	NA	NA	NA	Self-injury	–	Hitting self-biting fingers
Seizure	–	–	NA	–	NA	–	–	–	+	–	+
Peripheral neuropathy	–	–	–	NA	NA	NA	NA	NA	NA	NA	NA
Facial dysmorphism	–	–	NA	NA	NA	NA	NA	NA	+	+	+
Hypomyelination	+	+	+	+	+	+	+	+	–	+	+
Abnormal corpus callosum	–	–	–	–	–	+	+	–	–	+	+
NCV	–	–	+	+	+	+	+	+	NA	NA	NA
BAEP	+	+	+	+	+	–	–	–	NA	+	NA
Others	–	–	–	–	–	–	–	–	Sleep disturbance	Hypersomnia	Poor sleep
Ref	the present study	the present study	Inoue et al.	Inoue et al.	Torisu et al.	Matsufuji et al.	Matsufuji et al.	Matsufuji et al.	Yamamoto et al.	Yamamoto et al.	Yamamoto et al.

Abbreviations: BAEP, brainstem auditory-evoked potentials; EONDT, early onset neurological disease trait; MCI, mild cognitive impairment; NA, not available; NCV, nerve conduction studies; SPG2, spastic paraplegia type 2.

Notably, the *MORF4L2* gene is located at Xq22.2, a region with abundant low copy repeats (LCRs), that can contribute to genomic rearrangements. Therefore, we further sought the possibility of potential causative CNV from the WES data. CNVs analysis by WES revealed a microdeletion at Xq22.2, which was further verified by LRS analysis with accurate breakpoint mapping.

Xq22.2 encompasses 38 annotated genes (GCRh38/hg38), including the *PLP1* gene. The mutations of *PLP1* gene cause a spectrum of *PLP1*-related disorders, with differences in age at onset, disease severity, brain MRI, and

electrophysiology. Duplications are the most common mutations, accounting for 60%–70% of *PLP1*-related disorders, and are linked to the classic PMD.¹⁰ Patients with point mutations of *PLP1* are associated with variable phenotypes, which range from clinically mild to severe form.¹¹ In contrast to duplications, deletions are significantly rare and smaller in size, especially in males. It is possible that large microdeletions are embryonic lethal and only carriers of small deletions can survive.¹² Our patients exhibited symptoms of lower limbs spastic paraplegia, motor development delay, intellectual disabilities,

Patient 4	Patient 5	Patient B	BAB2595	BAB2650	BAB8120	BAB12522	BAB8201	BAB8204
Unclassified	Unclassified	SPG2	EONDT	EONDT	EONDT	EONDT	SPG2	SPG2
Female	Female	Male	Female	Female	Female	Female	Male	Male
1	7	16	13	9	3.5	8	15	16
–	–	+	+	+	+	+	+	+
Severe delay	Severe delay	NA	Severe delay	Severe delay	Severe delay	Severe delay	–	–
Mild delay	Severe delay	Delay	Severe delay	Severe delay	Severe delay	Severe delay	Severe delay	Severe delay
–	Strabismus	Nystagmus	Strabismus	Strabismus, nystagmus	Strabismus	Strabismus, left amblyopia, optic atrophy	Strabismus	Strabismus
Gastroesophageal reflux	–	NA	Gastroesophageal reflux disease, constipation	Gastroesophageal reflux disease	Gastroesophageal reflux disease	Gastroesophageal reflux disease, constipation	Poor appetite, G-tube	Gastroesophageal reflux disease
+	+	+	NA	NA	NA	NA	NA	NA
–	–	NA	NA	NA	NA	NA	NA	NA
NA	NA	NA	NA	NA	NA	NA	NA	NA
–	Repetitive hands to mouth	NA	–	–	Dystonia with occasional stereotyped behavior and tongue protrusion	hand-to-mouth and hand wringing stereotypies, irritable	–	–
–	–	–	–	–	–	+	–	–
NA	NA	NA	–	–	–	–	+	–
–	–	NA	–	+	+	–	–	–
NA	+	+	+	+	+	+	+	+
NA	–	–	–	+	–	+	+	–
NA	NA	NA	NA	NA	NA	NA	NA	NA
NA	NA	+	–	–	+	–	+	NA
Poor sleep	Impaired pain perception.	–	–	–	–	Ventricular septal defect, decreased bone mineral density, hypothyroidism	Peripheral neuropathy	–
Yamamoto et al.	Yamamoto et al.	Prior et al.	Hijazi et al.	Hijazi et al.	Hijazi et al.	Hijazi et al.	Hijazi et al.	Hijazi et al.

and ataxia, which were consistent with SPG2. Notably, recent studies have proposed a novel disease known as “hypomyelination of early myelinating structures (HEMS)”. It is caused by mutations in intron 3 or exon 3B, which lead to altered alternative splicing of PLP1/DM20 and subsequent reduction in the PLP1/DM20 ratio.^{13,14} Individuals affected by HEMS exhibited brain MRI images showing poor myelination in structures that are normally myelinated during the early stages, such as the brainstem, hilus of the dentate nucleus, posterior limb of internal capsule (PLIC), and optic tracts.^{7,14–16}

Conversely, patients with SPG2 exhibit the opposite MRI results, characterized by relatively inadequate myelination of structures that undergo myelination at a later age. This finding is similar to what was observed in our patients. Additionally, we performed Sanger sequencing on III-1, III-2, and II-5 to further exclude HEMS (Fig. 3D).

Until now, there are 20 reported patients with null PLP1 mutation, of which 11 were classified as SPG2, 7 presented as early-onset neurological disease trait (EONDT), and 2 were unclassified^{12,17–22} (Table 2). In these patients, motor development delay is the most

common symptom (19 out of 20, 95%), followed by intellectual development/cognitive function (13 out of 16, 81.3%), and spasticity (15 out of 20, 75%). All 11 SPG2 patients presented hypomyelination in brain MRI, with or without a thin corpus callosum. While peripheral neuropathy symptoms were reported in only one SPG2 patient (1 out of 5, 20%), decreased conduction velocities were observed in five patients (5 out of 7, 71.4%), and the remaining two patients exhibited normal nerve conduction velocities from our study. Compared to other null *PLP1* cases, the clinical features of patients in our study were relatively milder. We found the sporadic paraplegia was limited to lower limbs, with moderate motor development and mild cognitive impairment. Peripheral neuropathy is commonly observed in patients with null mutations. Interestingly, the patients in this study did not exhibit any features of peripheral neuropathy and had normal nerve conduction velocities. Analysis of BAEP revealed reduced amplitude and prolonged central conduction time (CCT). Additionally, hypomyelination was observed in the majority of white matter areas. These findings suggest that this microdeletion primarily affects central nervous system (CNS) while sparing the peripheral nervous system (PNS).

The genomic arrangement at Xq22.2 involving *PLP1* is a nonrecurrent event, and none of the published families

showed the same Xq22-*PLP1* deletion (Fig. 4). All previously reported patients presented with SPG2 had a full or partial deletion of *PLP1* (Table 3). However, the deletion in our patients was located ~658 kb away from *PLP1* gene. Therefore, it is unlikely that the associated clinical features were caused by loss or alterations in the coding regions of the *PLP1* gene. In the deletion region, we identified only the *GLRA4* and *TMEM31* genes, as well as the *MORF4L2* gene antisense RNA (*MORF4L2-AS*). *GLRA4* is a pseudogene and lacks the fourth transmembrane domain, while *TMEM31* encodes transmembrane protein 3, which has limited available information. Hence, it is also unlikely that these genes contribute to the SPG2 phenotype. Recently, Kim et al. uncovered two distal *PLP1* enhancers, EC1 and EC2, located between *MORF4L2* and *GLRA4*. Silencing either EC1 or EC2 resulted in a 47%–62% decrease in *PLP1* expression compared to Scr1, and silencing both EC1 and EC2 resulted in greater suppression of *PLP1* expression.⁸ Our study found the deletion located at chrX:103,690,507–103,715,018 (hg38) contains the both enhancers. Advanced experimental validation showed that EC1 and EC2 are oligodendrocyte-specific enhancers among various brain cells. The electromyography analysis of our patients strongly supports the notion that EC1 and EC2 play a crucial role in oligodendrocytes. It is noteworthy that the contribution of enhancers to

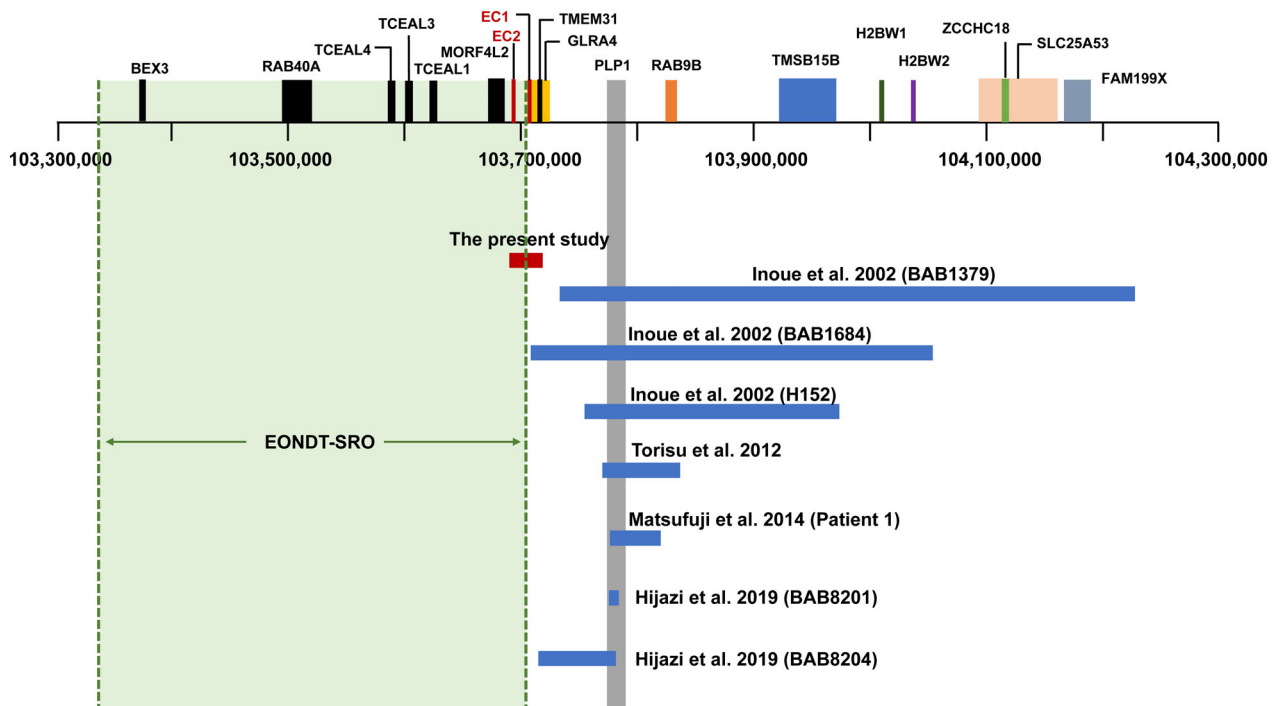


Figure 4. Results of deletions mapping at Xq22. The EONDT-SRO is shown in the green box. The blue and red bars indicated the deletion regions identified in patients with SPG2 phenotype.

Table 3. The summary of molecular features of patients with Xq22.2 large deletion.

Patient ID	Gender	Current age	Region (GRCh38/hg38) ^a	Junction features	Deletion size (Mb)	Inheritance	Classified type	Ref	Method
Proband (III-1)	M	18	chrX:103,690,507–103,715,018	5 bp microhomology	0.025	Maternal	SPG2	Present study	LRS
BAB1379	M	10	chrX:103,738,806–104,2654,06	18 bp microhomology	0.516	Maternal	SPG2	Inoue et al. ¹²	STS-content PCR, FISH
BAB1684	M	10	chrX:103,702,356–104,059,690	12 bp insertion	0.357	Maternal	SPG2	Inoue et al. ¹²	STS-content PCR, FISH
H152	NA	NA	chrX:103,754,900–103,960,308	32 bp insertion, 2 bp microhomology	0.205	Maternal	SPG2	Raskind et al. ¹⁹ and Inoue et al. ¹²	STS-content PCR, FISH
Patient A	M	2	chrX:103,764,022–103,837,108	1 bp microhomology	0.073	Maternal	SPG2	Toritsu et al. ³¹	STS-content PCR
Proband (II-1)	M	29	chrX:103,778,404–103,811,969	2 bp microhomology	0.033	Maternal	SPG2	Matsufuji et al. ²¹	MLPA, STS-content PCR
Patient 1	F	3	chrX:102,110,889–106,603,806	NA	4.481	De novo	EONDT	Yamamoto et al. ¹⁷	Microarray, FISH
Patient 2	F	7	chrX:101,404,127–106,280,373	NA	4.864	De novo	EONDT	Yamamoto et al. ¹⁷	Microarray
Patient 3	F	19	chrX:101,652,897–104,737,588	NA	3.074	De novo	EONDT	Yamamoto et al. ¹⁷	Microarray
Patient 4	F	1	chrX:102,727,936–102,978,598	NA	0.251	De novo	Unclassified	Yamamoto et al. ¹⁷	Microarray
Patient 5	F	7	chrX:103,704,530–103,789,615	NA	0.085	De novo	Unclassified	Yamamoto et al. ¹²	Microarray, FISH
Patient B	M	16	NA	Microhomology	0.018	NA	SPG2	Prior et al. ²²	MLPA
BAB2595	F	13	chrX:101,611,623–104,167,299	2 bp microhomology	2.545	De novo	EONDT	Hijazi et al. ¹⁸	Microarray
BAB2650	F	9	chrX:103,360,712–104,054,938	3 bp microhomology	0.694	De novo	EONDT	Hijazi et al. ¹⁸	Microarray
BAB8120	F	3.5	chrX:101,774,675–107,459,554	22 bp insertion 5 bp direct-repeat	5.673	De novo	EONDT	Hijazi et al. ¹⁸	Microarray
BAB12522	F	8	chrX:102,811,421–106,165,829	127 bp microhomology LINE-LINE	3.343	De novo	EONDT	Hijazi et al. ¹⁸	Microarray
BAB2614	F	NA	chrX:103,181,796–106,277,389	2 bp microhomology Alu-Alu	3.083	NA	NA	Hijazi et al. ¹⁸	Microarray
BAB8201	M	15	chrX:103,774,844–103,781,620	None	0.0067	Maternal	SPG2	Hijazi et al. ¹⁸	Microarray
BAB8204	M	16	chrX:103,712,368–103,783,677	1 bp microhomology	0.071	NA	SPG2	Hijazi et al. ¹⁸	Microarray
BAB2615	M	NA	chrX:103,288,544–104,153,553	1 bp microhomology	0.854	NA	NA	Hijazi et al. ¹⁸	Microarray

Abbreviations: EONDT, early onset neurological disease trait; FISH, fluorescent in situ hybridization; LRS, long-read sequencing; MLPA, multiplex ligation-dependent probe amplification; PCR, polymerase chain reaction; RT-PCR, reverse transcript-PCR; SPG2, spastic paraplegia type 2; STS-PCR, sequence-tagged sites-content PCR.
^aThe regions of previous study were transformed to GRCh38/hg38.

PLP1 transcription in Schwann cells may be relatively modest, as it does not result in a significant destabilization of peripheral myelin. However, further investigation is necessary to elucidate the underlying mechanism. Another possible cause is that the deletion at chrX:103,690,507–103,715,018 (hg38) may regulate the expression level of the *PLP1* gene through a position effect. Lee et al. reported a case of SPG2 with 135 to 185 kb downstream duplication of *PLP1* gene, suggesting that the duplication may lead to silencing of the *PLP1* gene through a position effect.²³ However, there was no associated mechanism proposed.

LRS enables the generation of reads exceeding 10 kb in length, and the PacBio platform offers high-fidelity reads with greater than 99% accuracy.²⁴ Recently, LRS has revealed tens of thousands of SVs of the genome and helped to solve several pathogenic mutations that have long gone unsolved.^{25–29} Previous studies have used traditional technical methods such as fluorescent in situ hybridization (FISH), multiplex ligation-dependent probe amplification (MLPA), or array comparative genomic hybridization (aCGH) to detect several SVs at Xq22. However, these methods did not provide information on the position of duplicated copies and were unable to resolve breakpoints at the nucleotide sequence level.³⁰ In this study, we used LRS whole genome sequencing to precisely map the deletion in the non-coding region and found a 5 bp microhomology at the breakpoint joint. Our study suggested that LRS is a powerful tool for detecting causal structural variants in genetic disorders.

Conclusions

In this study, we identified a novel microdeletion (about 24.5 kb) at Xq22.2 in a Chinese SPG2 family by WES and LRS, and it is the first report of SPG2 caused by the deletion of distal enhancers of *PLP1* gene. The lack of distal enhancers may result in transcriptional repression of *PLP1* in oligodendrocytes, potentially affecting its role in the maintenance of myelin, and causing SPG2 phenotype. This study has highlighted the importance of noncoding genomic alterations in the genetic etiology of SPG2.

Author contributions

Qiyang Sun and Sheng Zeng had full access to all of the data in the study and take responsibility for the integrity of the data and the accuracy of the data analysis. Concept and design: Qiyang Sun, Sheng Zeng, and Tang Beisha. Acquisition, analysis, or interpretation of data: Xun Zhou, Yige Wang, Runcheng He, Zhenhua Liu, Qian Xu,

Jifeng Guo, Xinxiang Yan, Jinchun Li, Tang Beisha, Sheng Zeng, and Qiyang Sun. Drafting of the manuscript: Qiyang Sun, Sheng Zeng, and Xun Zhou. Critical revision of the manuscript for important intellectual content: Qiyang Sun, Sheng Zeng, Jifeng Guo, and Tang Beisha. Statistical analysis: Xun Zhou and Sheng Zeng. Obtained funding: Sheng Zeng, Qiyang Sun, and Tang Beisha. Administrative, technical, or material support: Jifeng Guo, Sheng Zeng, and Tang Beisha. Supervision: Qiyang Sun and Sheng Zeng.

Acknowledgments

We are indebted to these participants for their generous participation in this study. This work was supported by grants from the National Natural Science Foundation of China (82171256, U20A20355, 82202051) and the Natural Science Foundation of Hunan Province, China (2021JJ31093, 2021JJ40819).

Conflict of interest statement

The authors have no conflict of interest to declare.

References

1. Ruano L, Melo C, Silva MC, Coutinho P. The global epidemiology of hereditary ataxia and spastic paraplegia: a systematic review of prevalence studies. *Neuroepidemiology*. 2014;42(3):174–183.
2. Harding AE. Classification of the hereditary ataxias and paraplegias. *Lancet* (London, England). 1983;1(8334):1151–1155.
3. Meyyazhagan A, Orlacchio A. Hereditary spastic paraplegia: an update. *Int J Mol Sci*. 2022;23(3):1697.
4. Blackstone C. Hereditary spastic paraplegia. *Handb Clin Neurol*. 2018;148:633–652.
5. Aggarwal S, Yurlova L, Simons M. Central nervous system myelin: structure, synthesis and assembly. *Trends Cell Biol*. 2011;21(10):585–593.
6. Osório MJ, Goldman SA. Neurogenetics of Pelizaeus-Merzbacher disease. *Handb Clin Neurol*. 2018;148:701–722.
7. Claringbould A, Zaugg JB. Enhancers in disease: molecular basis and emerging treatment strategies. *Trends Mol Med*. 2021;27(11):1060–1073.
8. Kim D, An H, Fan C, Park Y. Identifying oligodendrocyte enhancers governing *Plp1* expression. *Hum Mol Genet*. 2021;30(23):2225–2239.
9. Li J, Zhao T, Zhang Y, et al. Performance evaluation of pathogenicity-computation methods for missense variants. *Nucleic Acids Res*. 2018 Sep 6;46(15):7793–7804.
10. Siermans EA, de Coo RF, De Wijs IJ, Van Oost BA. Duplication of the proteolipid protein gene is the major

- cause of Pelizaeus-Merzbacher disease. *Neurology*. 1998;50(6):1749-1754.
11. Cailloux F, Gauthier-Barichard F, Mimault C, et al. Genotype-phenotype correlation in inherited brain myelination defects due to proteolipid protein gene mutations. *Clinical European Network on Brain Dysmyelinating Disease. Eur J Human Genet*. 2000;8(11):837-845.
 12. Inoue K, Osaka H, Thurston VC, et al. Genomic rearrangements resulting in PLP1 deletion occur by nonhomologous end joining and cause different dysmyelinating phenotypes in males and females. *Am J Hum Genet*. 2002;71(4):838-853.
 13. Nicita F, Aiello C, Vasco G, et al. Expanding the clinical and mutational Spectrum of the PLP1-related Hypomyelination of early myelinated structures (HEMS). *Brain Sci*. 2021;11(1):93.
 14. Kevelam SH, Taube JR, van Spaendonk RM, et al. Altered PLP1 splicing causes hypomyelination of early myelinating structures. *Ann Clin Transl Neurol*. 2015;2(6):648-661.
 15. Tonduti D, Pichiecchio A, Wolf NI, et al. Novel hypomyelinating leukoencephalopathy affecting early myelinating structures: clinical course in two brothers. *Neuropediatrics*. 2013;44(4):213-217.
 16. Steenweg ME, Wolf NI, Schieving JH, et al. Novel hypomyelinating leukoencephalopathy affecting early myelinating structures. *Arch Neurol*. 2012;69(1):125-128.
 17. Yamamoto T, Wilsdon A, Joss S, et al. An emerging phenotype of Xq22 microdeletions in females with severe intellectual disability, hypotonia and behavioral abnormalities. *J Hum Genet*. 2014;59(6):300-306.
 18. Hijazi H, Coelho FS, Gonzaga-Jauregui C, et al. Xq22 deletions and correlation with distinct neurological disease traits in females: further evidence for a contiguous gene syndrome. *Hum Mutat*. 2020;41(1):150-168.
 19. Raskind WH, Williams CA, Hudson LD, Bird TD. Complete deletion of the proteolipid protein gene (PLP) in a family with X-linked Pelizaeus-Merzbacher disease. *Am J Hum Genet*. 1991;49(6):1355-1360.
 20. Grossi S, Regis S, Biancheri R, et al. Molecular genetic analysis of the PLP1 gene in 38 families with PLP1-related disorders: identification and functional characterization of 11 novel PLP1 mutations. *Orphanet J Rare Dis*. 2011;6:40.
 21. Matsufuji M, Osaka H, Gotoh L, Shimbo H, Takashima S, Inoue K. Partial PLP1 deletion causing X-linked dominant spastic paraplegia type 2. *Pediatr Neurol*. 2013;49(6):477-481.
 22. Prior C, Muñoz-Calero M, Gómez-Gonzalez C, et al. A novel PLP1 deletion causing classic Pelizaeus-Merzbacher disease. *J Neurol Sci*. 2019;397:135-137.
 23. Lee JA, Madrid RE, Sperle K, et al. Spastic paraplegia type 2 associated with axonal neuropathy and apparent PLP1 position effect. *Ann Neurol*. 2006;59(2):398-403.
 24. Logsdon GA, Vollger MR, Eichler EE. Long-read human genome sequencing and its applications. *Nat Rev Genet*. 2020;21(10):597-614.
 25. Beyter D, Ingimundardottir H, Oddsson A, et al. Long-read sequencing of 3,622 Icelanders provides insight into the role of structural variants in human diseases and other traits. *Nat Genet*. 2021;53(6):779-786.
 26. Sun QY, Xu Q, Tian Y, et al. Expansion of GGC repeat in the human-specific NOTCH2NLC gene is associated with essential tremor. *Brain J Neurol*. 2020;143(1):222-233.
 27. Tian Y, Wang JL, Huang W, et al. Expansion of human-specific GGC repeat in neuronal Intranuclear inclusion disease-related disorders. *Am J Hum Genet*. 2019;105(1):166-176.
 28. Zeng S, Zhang MY, Wang XJ, et al. Long-read sequencing identified intronic repeat expansions in SAMD12 from Chinese pedigrees affected with familial cortical myoclonic tremor with epilepsy. *J Med Genet*. 2019;56(4):265-270.
 29. Merker JD, Wenger AM, Sneddon T, et al. Long-read genome sequencing identifies causal structural variation in a Mendelian disease. *Genet Med*. 2018 Jan;20(1):159-163.
 30. Alkan C, Coe BP, Eichler EE. Genome structural variation discovery and genotyping. *Nat Rev Genet*. 2011;12(5):363-376.
 31. Torisu H, Iwaki A, Takeshita K, et al. Clinical and genetic characterization of a 2-year-old boy with complete PLP1 deletion. *Brain & development*. 2012 Nov;34(10):852-856.

Supporting Information

Additional supporting information may be found online in the Supporting Information section at the end of the article.

Supplemental Figure 1 Integrative Genomics Viewer (IGV) visualization of BAM files showed large hemizygous deletion in III-1 and III-2 (red box), and a possibly heterozygous deletion in II-5 according to the sequencing depth (red arrow) compared to her mother (I-4).